AJP

ISSN : 0971 - 3093

Vol 30, No 2, February, 2021

ASIAN JOURNAL OF PHYSICS

An International Peer Reviewed Research Journal

Advisory Editors : W. Kiefer & FTS Yu

W Kiefer in ELARS during Corona times

ANITA PUBLICATIONS

FF-43, 1st Floor, Mangal Bazar, Laxmi Nagar, Delhi-110 092, India

B O : 2, Pasha Court, Williamsville, New York-14221-1776, USA

Asian Journal of Physics
Vol. 30, No 2 (2021) 281-301
Available on: www.asianjournalofphysics.in

ap

Immuno-SERS microscopy: From SERS nanotag design and correlative single-particle spectroscopy to protein localization on single cells and tissue

Michelle Hechler, Supriya Srivastav and Sebastian Schlücker*
Department of Chemistry and Center for Nanointegration Duisburg-Essen (CENIDE), University Duisburg-Essen, Universitätsstr. 5, 45141 Essen, Germany

This review summarizes work from the authors' laboratory on immuno-surface-enhanced Raman scattering (iSERS) microscopy since the demonstration of its proof of concept in 2006. iSERS microscopy is an emerging bioimaging technique for the selective localization of proteins on single cells and tissue. Selectivity for target proteins is achieved by labeling the corresponding antibodies with SERS labels/nanotags, i.e., molecularly functionalized noble metal nanoparticles for spectral identification. Central advantages of iSERS are multiplexing, quantification, minimization of autofluorescence, no/minimal photobleaching and the need for only a single laser excitation wavelength. The performance of SERS labels/nanotags can be studied in correlative single-particle SERS microspectroscopic and electron microscopic experiments. The rational design of optimal SERS labels/nanotags can be supported by computer simulations predicting the optical properties including the SERS signal enhancement. Work on iSERS from the authors' group over the past 15 years on the selective localization of target proteins, especially in cancer diagnostics, on tissue and single cells is highlighted.

Keywords: iSERS microscopy, SERS labels/nanotags, (iSECARS), Bioimaging technique.

1 Introduction

Immuno-SERS (SERS: surface-enhanced Raman scattering) microscopy is a novel imaging technique for protein localization on cells and tissue specimen [1]. Based on current medical practice like immunohistochemistry (IHC) and immunofluorescence (IF), the targeted protein is recognized by a labeled antibody for localization [2,3]. In immuno-SERS (iSERS) microscopy, the utilized antibodies are conjugated to molecularly functionalized noble metal colloids, i.e. gold or silver metal nanoparticles (NPs) with organic Raman-active molecules (Raman reporters) chemisorbed on their surface [4-6], forming the so-called SERS label/nanotag (Fig 1).

The Raman reporter molecules have a unique vibrational Raman spectrum and therefore provide characteristic spectral barcodes for the identification and quantification of each label, while the metal NPs provide the necessary signal enhancement upon excitation of a localized surface plasmon [8]. SERS combines the benefits of Raman spectroscopy like abundant spectral information and, especially important for biological samples, low water interference while overcoming the obstacle of low sensitivity. Raman signal enhancement can be increased by positioning reporters in "hot spots" generated at NP tips, edges and inter-particle junctions [9]. The rational design of the SERS nanotag regarding size, shape and chemical composition strongly influence the SERS enhancement [8].

Central advantages of iSERS over immuno-based protein localization methods like IF and IHC include the possibility of quantification due to the molecular fingerprint intensity of Raman reporters [10],

Corresponding author
e-mail: sebastian.schlücker@uni-due.de (Sebastian Schlücker)

a single laser excitation wavelength for all SERS nanotags, utilization of red to near-infrared excitation wavelengths to minimize autofluorescence of the analyzed samples, no bleaching of SERS nanotags and the enormous multiplexing capacity for simultaneous target detection because of the narrow line width of vibrational vibrational Raman bands. For example, Schütz and Schlücker have demonstrated a quantitative 6-plex SERS experiment with 6 spectrally distinct SERS nanotags by using various mixtures of them [11]. However, a disadvantage of SERS labels is their large size and weight compared to molecular fluorophores and enzymes. This aspect strongly impairs iSERS suitability for live cell imaging, but not for the detection of cell surface antigens or their use in assays, such as lateral flow assays [12]. In addition to iSERS based on surface-enhanced spontaneous Raman scattering also the corresponding nonlinear Raman technique, immune surface-enhanced coherent anti-Stokes Raman scattering (iSECARS) has been demonstrated in 2011 by our group together with the IPHT in Jena, Germany [13].

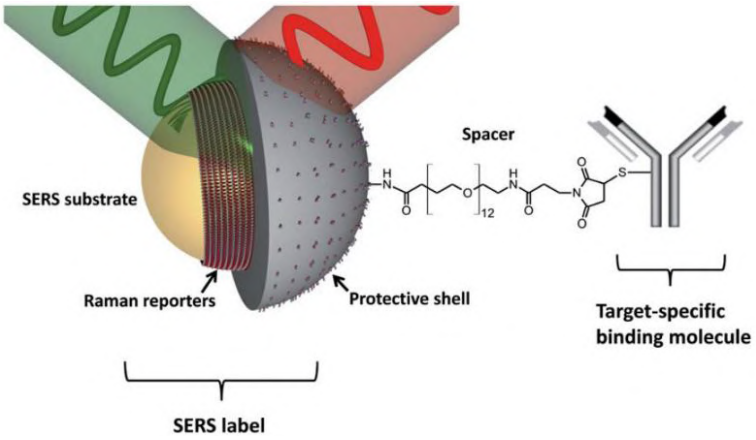

Fig 1. Composition of a SERS label/nanotag for iSERS microscopy: the SERS substrate (plasmonically active gold nanoparticle), covered with Raman reporter molecules adsorbed on its surface, surrounded by an optional protective layer (in this image depicted as a glass shell). This SERS label is bioconjugated to the target-recognizing antibody by a spacer molecule. From ref [7].

Due to its high sensitivity and molecular fingerprint specificity, a lot of attention has been given to make iSERS suitable for selective protein localization [1]. In this review, we summarize work from the authors' laboratory since the proof of principle of iSERS microscopy in 2006. We begin with the design of SERS labels/nanotags, their characterization at the single-particle level in correlative SERS/SEM experiments and their application to iSERS microscopy for protein localization on tissues and single cells.

2 Development of SERS nanotags suitable for bioanalytical and biomedical applications

The proof of principle experiments regarding protein detection in solution with Raman reporter-functionalized gold NPs conjugated to immunoglobuline G were performed as a sandwich assay by Porter and co-workers in 1999 [14]. 30 nm gold NPs were coated with thiophenol (TP), 2-naphthalenethiol (NT), and 4-mercaptobenzoic acid (4-MBA) as Raman reporter molecules and subsequently linked to the amines of anti-rat- or anti-rabbit-immunoglobulin G through ionic and hydrophobic interactions within 60 min incubation time at room temperature. Glass slides were coated with gold to immobilize the same antibodies bound to the used NPs for subsequent antigen-binding (free rat or rabbit IgG). With an integration time of 1 s a detection limit of about 30 ng/mL (0.2 nM) was estimated for the used antigens. Moreover, simultaneous detection of two different analytes (rat and rabbit IgG) could be demonstrated successfully [14].

2.1 First in situ detection of PSA with iSERS microscopy

The first demonstration to detect antigens with immuno-Raman microspectroscopy *in situ* in tissue specimen was published by Schlücker and co-workers in 2006 [15]. In this study, it was possible to detect a tumor marker for prostate cancer, prostate-specific antigen (PSA), with high selectivity and sensitivity in 5 µm thick FFPE tissue specimen of patients with prostate carcinoma. Antigens on the tissue surface were retrieved by heat-induced epitope retrieval (HIER). The Raman reporter 5,5'-dithiobis (succinimidyl-2-nitrobenzoate) was synthesized and covalently linked to hollow gold/silver nanoshells and a PSA antibody. With a laser power of 1 mW and an acquisition time of 5 s, selective detection of PSA could be demonstrated [15].

Experiments like this built the foundation for the following years of research invested in SERS nanotags improvements, which should lead to a reduction of acquisition time and necessary laser power as well as increased stability of the labels to ensure reproducibility. In achieving these aims a technique potent enough to compete with IF or IHC should be created. Using SERS nanotags that emit strong and small vibrational Raman peaks enabled multiplexing experiments with up to six colors, which is a striking advantage e.g. compared to the ~4 colors usually used in IHC/IF [11,16].

2.2 SERS nanotags for red laser excitation

For successful application of SERS nanotags in the medical field, the rational design of the SERS label with specified physical and chemical properties is crucial. This includes i) sensitivity: the Raman signal enhancement from the plasmonic nanoparticle which determines the detect limit and the acquisition time in imaging experiments; ii) multiplexing: the line width and the number of vibrational bands of the Raman reporter determines the maximum number of spectral barcodes spectrally discriminated and thereby the maximum number of target proteins which can be simultaneously localized on the same specimen; iii) stability: the Raman reporter and an optional protective shell determine the colloidal stability which is highly important for avoiding aggregation during the course of the experiments; iv) reproducibility: synthesizing a colloid with a defined composition of particles, i.e. uniform SERS nanotags is important for obtaining reproducible iSERS results. Overall, obtaining reliable iSERS results necessitates the use of stable and uniform SERS nanotags, which requires synthetic and purification efforts [7].

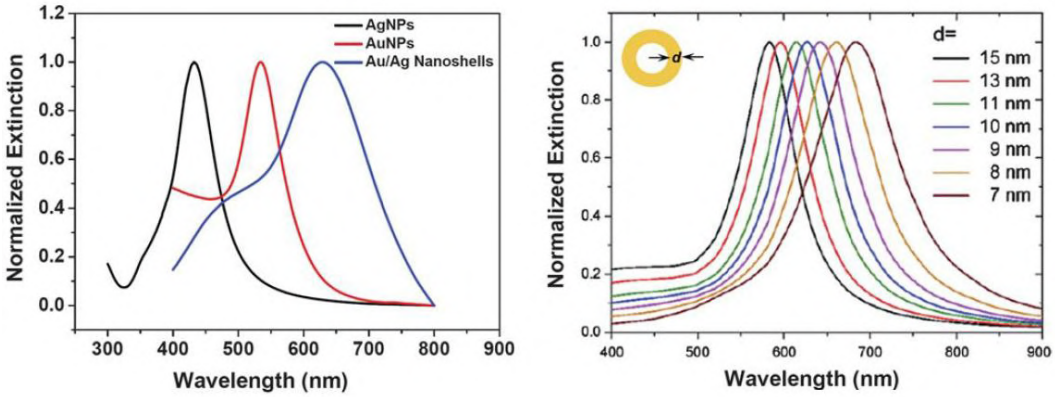

Fig 2. Left: Experimental extinction spectra of AgNPs, AuNPs and gold/silver nanoshells in water. Right: Calculated extinction spectra of single gold/silver nanoshells with a radius of 27.5 nm and different shell diameters. From ref. [7].

Firstly, the choice of the metal colloid with desired properties, e.g. the position of the localized surface plasmon resonance (LSPR) peak and achievable signal enhancement, has to be made. The position of the LSPR peak depends on the size and shape of the NP, the dielectric function of the metal as well as that of the surrounding medium [9]. Silver and gold NPs exhibit LSPR peak in the blue and green, respectively

(Fig 2 left). For biological specimen using excitation wavelengths in this spectral region is often accompanied by disturbing autofluorescence which may mask the Raman contribution in the corresponding image. Therefore, our group initially focused on gold/silver nanoshells for red laser excitation [17]. This requires the use of tailor-made plasmonic NPs with LSPR peaks in the red for red laser excitation for minimizing the disturbing autofluorescence from the biological specimen. Hollow spheres comprising a shell of silver and gold, also called gold/silver nanoshells, exhibit an LSPR peak which can be tuned across the red to near infra-red region, depending on the NP size and shell thickness (Fig 2 right).

Secondly, the choice for the class of Raman reporters has to be made. Our group focused on the use of aromatic thiols as Raman reporters which form self-assembled monolayers (SAMs) on gold surfaces such as ca. 60 nm large gold nanoshells (Fig 3) [15]. Benefits of such a SAM are elimination or minimization of undesirable molecules coadsorbing on the NP surface, hence avoiding spectral interference, as well as optimal coverage with the chosen reporter molecule in order to maximize SERS intensity. The uniform orientation of the Raman reporter molecules relative to the NP surface decreases the line broadening of the detected Raman bands. This ensures spectral reproducibility and provides the possibility for spectral multiplexing [2]. Critical issues are particle aggregation when the SAM does not sufficiently stabilize the SERS label/nanotag as well as the desorption of Raman reporter molecules from the surface caused by stronger interactions between the SAM and the solvent environment.

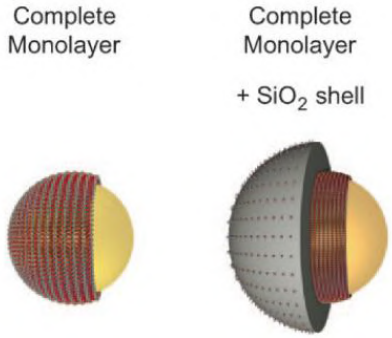

Fig 3. Single SERS nanoparticles with and without encapsulation. Left: Complete monolayer without protective encapsulation. Right: Complete monolayer coverage with protective silica shell. From ref. [2].

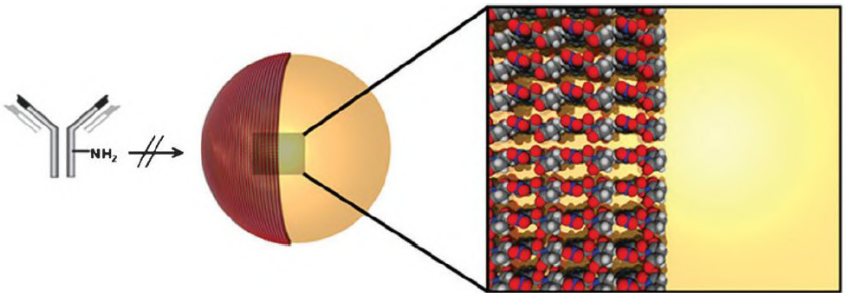

Fig 4. Conjugating the antibody to the metal nanoparticle is impaired by the dense and uniform packing of Raman reporters as a SAM on the surface of the nanoparticle. From ref [20].

These obstacles can be overcome by encapsulating NPs surrounded by a SAM with a silica shell to increase their chemical and mechanical stability. To this end, the SAM was first coated with poly(allylamine hydrochloride), followed by a layer of polyvinylpyrrolidone. Then a mixture of ammonia and tetraethylorthosilicate in 2-propanol lead to a growing silica shell (modified Stöber method) [18]. The

reproducibility of this method was proven by TEM analysis of silica-encapsulated gold/silver nanoshells. Compared to submonolayer coverage with Raman reporters, NPs with a SAM displayed SERS signals that were 22 times higher [19].

In addition to this 2-step procedure, comprising the addition of the Raman reporter followed by the time-consuming addition of two polyelectrolytes before the actual silane, Schütz *et al* group also developed a direct route to silica encapsulation by integrating the Raman reporter and a silane anchor into a single molecular entity via covalent chemistry [19]. Also, a non-covalent approach using noncavlently bound silence precursors was developed [21].

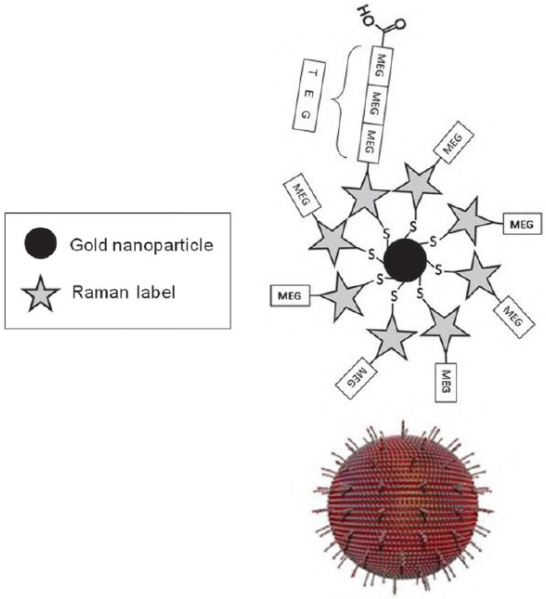

Fig 5. Dual SAM design for water soluble SERS nanotags stabilized by two hydrophilic SAM components: Conjugation of hydrophilic mono- and triethylene glycol units to the Raman reporter molecules stabilizing the SAM. The terminal carboxylic acid for bioconjugation is depicted. From ref. [20]

To increase the biocompatibility of the SERS nanotag, another synthesis route for an encapsulating shell around the NP was tested [20]. A synthesis of silver/gold nanoshells with attachment of hydrophilic monoethylene glycol (MEG) containing a terminal hyrdroxyl group to ensure water solubility of the stabilizing shell of the SERS nanotag was performed. Moreover, a mixture of MEG and triethylene glycol (TEG) containing a terminal carboxyl moiety for bioconjugation to amines of the applied antibodies were used (Fig 5). TEG served as a spacer between the surface of the SERS nanotag and the antibody, as the bioconjugation directly onto a SAM is sterically impaired by the dense packing of Raman reporter molecules (Fig 4) [22]. Bioconjugation could be controlled by varying the ratio between MEG and TEG. In the conducted experiments a ratio of 1000:1 (MEG-OH:TEG-COOH) exhibited successful NP-antibody conjugation. Formation of a SAM slightly shifted the plasmon band compared to bare NPs about 20 nm into the red. After bioconjugation with NHS ester chemistry no further shift was detected. An excitation wavelength in the red to near-infrared spectrum is beneficial for SERS microscopy, as it minimizes the influence of autofluorescence during measurements. All SERS spectra displayed similar signal-to-noise ratios (if concentration-dependent effects are neglected), rendering this synthesis route suitable for multiplexing experiments. This approach was repeated with 60 nm gold nanostars, which were synthesized in an aqueous medium using sodium citrate

as a reducing agent. The development of a synthesis route for monodisperse gold nanostars in water further increased the biocompatibility of the SERS nanotags, as organic substances like CTAB and DMF, which denature proteins, could be avoided. Moreover, in the presented experimental setup silver nanoparticles exhibit oxidation. Therefore, NPs consisting of gold are preferred due to their chemical inertia, even though they are less plasmonically active than silver or gold/silver NPs [20].

2.3 Assessing the SERS brightness of different NPs in single-particle experiments and simulations

Since the dominant contribution of the increased Raman signal intensities in SERS compared to conventional Raman spectroscopy stems from the electromagnetic enhancement, investigating which metal structures provide the strongest enhancement according to their plasmon resonance is necessary to achieve Raman signals strong enough for single-particle analysis. Previous studies reported e.g. that SERS signal intensities of symmetric particles are four times higher than their asymmetric counterparts (Niu *et al*) [23]. Ling and coworkers examined the effect of modifications like etching on NP surfaces and stated, that their modified structures emitted 30 times higher signals than the original ones [24]. Size also affects SERS signal intensity: Lin and coworkers analyzed gold nanorods with the same LSPR wavelength but different sizes. The smaller nanorods displayed stronger SERS enhancements than the bigger ones [25]. Investigating the size effect with colloid NPs was proven to be challenging as the geometry of the particle strongly influences the signal enhancement and monodispersed spherical Au NPs did not provide sufficient signal intensities at the single-particle level [26,27].

In addition to the initial use of gold/silver nanoshells in our group, we then moved on to core/satellites structures, which benefit from very high electric field enhancements occurring in the short (1-2 nm) gaps between the particles. In this context, different approaches to core/satellite SERS tags were used, for example, by using a thiol-modified ultrathin silica shell on the core particle or a molecular linker for electrostatic assembly of the satellites to the core [28]. Both of these particle assembly-approaches result in exhibiting single-particle SERS brightness in correlative SERS/SEM experiments. Later this concept was modified and extended to the design of core/satellite particle for label-free monitoring of catalyzed chemical reactions on gold/gold [29] and silver/silver [30] superstructures .

Dimers and trimers of noble metal NPs are the smallest possible structures which benefit from the immense electric field enhancement arising from plasmonic coupling between the building blocks. While monomers are not-SERS active at the single-particle level, dimers and trimers are [31].

In order to evaluate the influence of the various previously reported contributing factors, a single-particle SERS study by Erni's and our group compared the SERS signal enhancements of different classes of NPs (Fig 6) [32]. Among the tested structures were a) gold NPs, b) quasi-spherical gold/silver hollow nanoshells, c) anisotropic gold nanostars containing tips with a high curvature radius and d) complex, but still quasi-isotropic gold core/satellite particles. To conduct correlative single-particle experiments, a highly diluted ethanol suspension of each of the NPs coated with 4-MBA was applied on a gold-framed silicon wafer. Isolated particles were identified with dark-field microscopy before confocal Raman microspectroscopy could be performed and SEM images were recorded subsequently. It was possible to assign single-NP SERS spectra to their corresponding structures.

The optical responses of the chosen NPs were calculated in computer simulations based on the finite-element method (FEM), which is particularly sophisticated when complex shaped NPs with highly dispersive material properties have to be analyzed [32]. However, optical responses of complex NPs like nanostars and supraparticles (core/satellite particles) still cannot be approximated well, as the lack of symmetry defines a unique configuration for each particle and each simulated optical NP response is highly context-dependent, making it nearly impossible to reproduce it experimentally. Therefore, simulations and experiments performed to determine optical responses of nanostars and supraparticles have to be averaged to be significant.

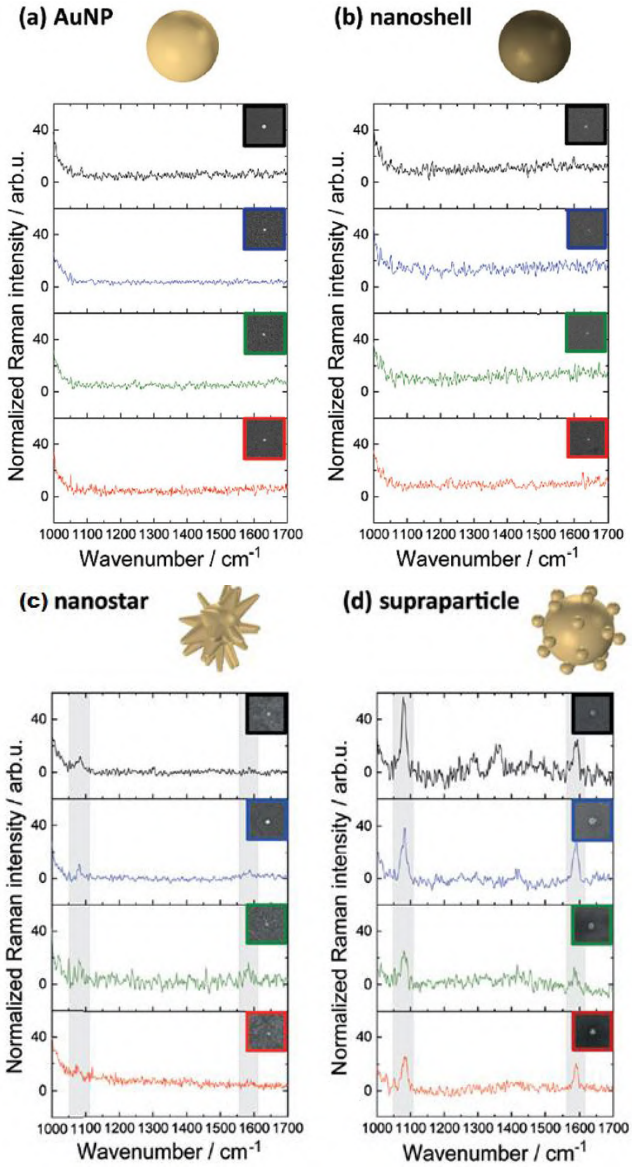

Fig 6. Results of correlative single-particle SERS/SEM experiments: SERS spectra and corresponding SEM images of monomers of (a) Au nanospheres, (b) gold/silver nanoshells, (c) gold nanostars and (d) gold supraparticles are depicted. From ref [32].

Correlative single-particle SERS/SEM experiments were performed with 4-MBA as the Raman reporter molecule. Using red laser excitation with a wavelength of 633 nm for the SERS mapping experiments with an integration time per pixel of 0.5s and a laser power of 220 µW, the gold NPs and gold/silver nanoshells did not exhibit detectable SERS signals. They were only detectable at the ensemble level in cuvette measurements of suspensions also containing clusters and larger aggregates. A Raman reporter exchange of 4-MBA to 4-NTB with a more intense nitro stretching peak compared to 4-MBA's phenyl bands did not result in Raman signals detectable at the single-particle level (Fig 6 a & b). On the other

hand, single gold nanostars and single gold core/satellite supraparticles exhibited detectable SERS signals (Fig 6 c & d). After normalization of the 4-MBA Raman bands at 1079 cm^{-1} to the silicon 1^{st}-order phonon Raman peak at 520 cm^{-1} as an internal standard, the SERS intensities from single gold nanostars vary between 11–14 counts while the SERS intensities of supraparticles vary between 26–59 counts. Electric field enhancements of modelled single particles were calculated for 633 nm laser excitation and averaged over the entire metal particle surface. FEM simulations for the examined NP types revealed highly localized electric field enhancement at the tips of the gold nanostars and in the particle junctions between core and satellites of the supraparticles. Due to the fact that the Raman reporter only binds to the surface of the satellites and not the core particle, calculations of the field enhancement omitted the junctions between them. In summary, this contribution examined the SERS brightness of different types of AuNPs at the single-particle level in simulations and correlative SERS/SEM experiments. It was concluded that spherical particles, single gold nanoshperes and gold/silver nanoshells do not exhibit detectable SERS signals at the single-particle level. Gold nanostars with strong electric field enhancement at their tips and core/satellite supraparticles showed detectable SERS signal intensities in experiments under the given conditions, therefore subsequent studies focused on these NPs [32].

2.4 Fast iSERS microscopy of prostate tissue with single gold NP dimers and trimers

In the iSERS staining experiments performed in the authors' laboratory before 2012, the Raman signal intensities of the SERS nanotags were not strong enough for detection in single-particle experiments using integration times of ca. 1s. Therefore, false-negative results could not be excluded: imagine, for example, a single SERS nanotags/antibody conjugate, which specifically binds to the antigen, but which cannot be detected due to its insufficient brightness. Moreover, stronger Raman signals open the possibility to reduce acquisition times per pixel and thus increase the area under investigation in the same overall acquisition time. Since dimers and trimers of noble metal NPs show a SERS enhancement several orders of magnitude higher than that of the monomers, due to the "hot spots" in the junctions between the single connected spheres, staining with these structures was tested and compared to the monomers [31]. The 60 nm nanoparticles were synthesized with bromo-mercaptobenzoic acid as the coating Raman reporter and subsequently encapsulated in a glass shell. Dimers and trimers were separated from monomers with density gradient centrifugation. High sample purity obtained by the separation method was proven by TEM analysis. UV/Vis extinction spectra of the separated colloids were acquired, revealing a plasmon peak at 542 nm in both samples, containing either monomers or dimers and trimers, and an additional peak at 690 nm for dimers and trimers. This peak belongs to the longitudinal mode along the axis between two spheres and can be excited with red laser radiation giving rise to a "hot spot" [9,32,33]. Single-particle SERS experiments were conducted by deposition of the colloids on a silicon wafer containing gold frames for orientation for correlation of dark field microscopy and SERS mapping. Due to the strong field enhancements of the dimers and trimers, the acquisition time in mapping mode was set to 30 ms per point. Single trimers yielded a SERS signal two to three times stronger than single dimers, only the glass-coated single monomers did not exhibit a detectable SERS signal. The higher signal intensity of the trimers can be explained by the larger number of hot spots, as well as the highly anisotropic response of the dimers [34,35].

To assess the utility of dimers and trimers for staining, the colloids were conjugated to anti-p63 antibody. p63 is a p53-homologue regulating differentiation, apoptosis and proliferation of epithelial cells. It is abundant in the cell membrane of healthy prostate cells in the basal epithelium. After paraffin removal and antigen retrieval on FFPE prostate tissue of healthy donors the tissue slides were incubated with SERS-labeled anti-p63 antibodies. Abundance of p63 only in the basal epithelium could be observed, while no signals were detected in the secretory epithelium and the stroma (Fig 7). The reduction from seconds employed in the initial iSERS study [15] to 30 ms acquisition time resulted in 33 times faster imaging of the corresponding tissue sections making SERS more suitable for histological analysis, when large areas of tissue have to be investigated.

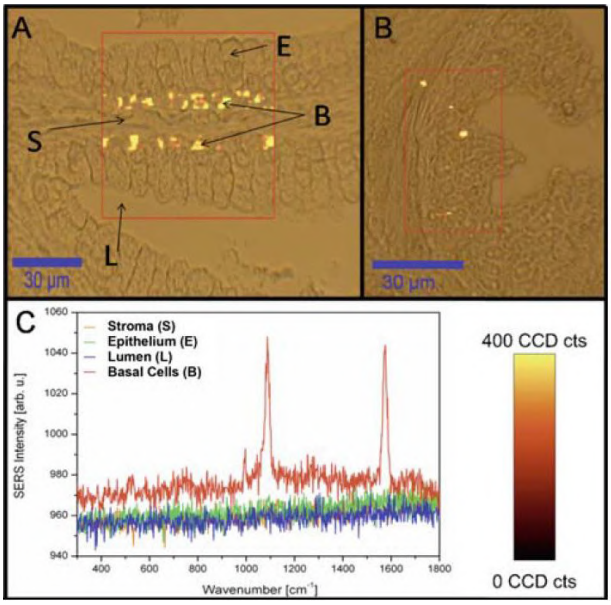

Fig 7. Immunohistochemistry on prostate tissue from healthy donors performed with anti-p63 antibody-SERS cluster conjugates with single-particle sensitivity. **A** White light image combined with a SERS false-color image exhibiting selective abundance of p63 in basal epithelial cells (B), E: non-basal epithelial cells, L: lumen of the prostatic gland, S: stroma. **B** White light image overlaid with a SERS false-color image of the negative control experiments with BSA conjugated to the SERS nanotag. **C** Representative SERS spectra measured at the locations indicated by arrows in **A**. From ref. [31]

Overall, the synthesis and purification of silica-encapsulated small clusters of gold NPs is quite time consuming. Therefore, our group later switched to PEGylated of plasmonic NPs such as gold nanostars [36–38] and gold/gold core/satellite NPs [12,16,39].

2.5 Organic synthesis of bright Raman reporters for tissue imaging via iSERS

Another approach to increase the signal intensity of the developed SERS nanotags is to design Raman reporters with strong and characteristic Raman bands for optical detection. Important features of ideal Raman reporters include as few vibrational Raman bands as possible and minimal band overlap for maximal multiplexing, as well as large scattering cross sections for high signal intensity. The number of vibrational modes is 3N–6 for nonlinear and 3N–5 for linear molecules with N atoms, therefore small molecules are preferred for multiplexing experiment. To achieve high signal brightness, Raman reporters containing highly polarizable moieties, e.g. double or triple bonds, are required [40]. For chemisorption of the Raman reporter molecules onto the surface of silver or gold NPs, functional groups containing heteroatoms like nitrogen and sulfur are favored [41]. Often derivatives of mercaptobenzoic acid (MBA) are used due to the highly polarizable π-electrons of the aromatic ring and the thiol group enabling the formation of a SAM on the NP surface [42]. In 2011, Lambert and co-workers synthesized Raman reporters with olefin and alkyne moieties [40]. Their goal was to control the characteristic wavenumber positions of the vibrational Raman bands by modification of the conjugation length and the substitution pattern of the Raman reporter molecules. Then hydrophilic stabilization and silica encapsulation had to be demonstrated, followed by bioconjugation to anti-p63 antibodies and staining experiments of p63 in prostate biopsies by iSERS microscopy. One molecule exhibited an exceptionally strong Raman band from a phenyl ring mode at about 1582 cm^{-1}. This compound, S-4-((4-(2-(2-hydroxyethoxy) ethylcarbamoyl)phenyl) ethynyl)phenyl ethanethioate (SEMA4),

was then chemisorbed onto the metal surface at its arene thiol. A thin silica shell coated the SERS label and the anti-p63 antibody was conjugated by standard EDC/s-NHS chemistry. The antigen p63 could be detected in the prostate basal epithelium [40]. Recently, our group synthesized a series of polyene-based Raman reporters with varying chain length for use in iSERS experiments [43].

2.6 Methods of bioconjugation

An important step before the actual staining iSERS microscopic imaging is the successful functionalization of the SERS nanotag with antibodies to ensure reliable binding to accessible antigens. Electrostatic interactions are one option to bind antibodies to the NP surface. Functional groups with positive charges are abundant in the peptide side chains of antibodies. These groups guide the ionic interaction with the (often negatively) charged NP surface. However, electrostatic/ionic interactions are non-covalent and reversible, therefore we focused on covalent conjugation techniques by EDC/sNHS-chemistry [44]. EDC reacts with the terminal carboxylic acid of the polymer coating the NP (carboxy-PEG) to form an amino-reactive ester intermediate. The efficiency of this coupling step is increased by the addition of sulfo-NHS, which yields an intermediate reacting with a random amino-group exposed on the surface of the antibody to form a stable amide bond [45]. A major drawback of this technique is the lack of selectivity since the active carboxylic acid can in principle react with every amino group of the antibody. For successful antigen recognition, presence of accessible flexible domains of the antibody is crucial, otherwise the binding site can be blocked leading to false-negative results. Other conventional bioconjugation schemes also do not include site-specific binding, therefore targeted amino groups can be conveniently close to the Fc part of the antibody or too close the antigen binding sites as well. To prevent the risk of synthesizing SERS nanotags without an accessible antigen recognition site, the chimeric protein A/G was employed. It exhibits selective binding to the Fc domain of antibodies. Coating the silica surface of the AuNP with this protein ensures antibody-binding with a free flexible domain (Fig 8) [46,47].

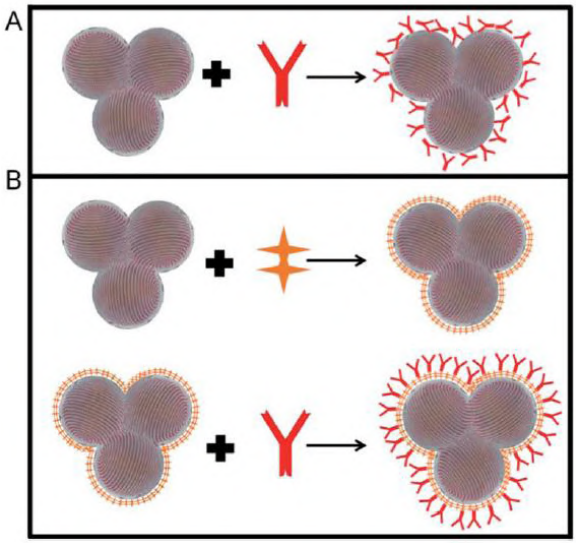

Fig 8. Conjugation of antibodies to silica-encapsulated clusters of gold NPs with single-particle sensitivity. **A** Uncontrolled binding of the antibody to the silica shell of the NP clusters. The random orientation of the bound antibodies may result in blocked antigen binding sites. **B** Coating of the silica surface of the SERS NP with protein A/G containing binding sites for the Fc fragment of the antibody (top). Controlled binding and a directed orientation of the antibodies on the NP cluster surface with accessible binding sites (bottom). From ref. [48].

3. iSERS microscopy with single-particle sensitivity on single cells and tissue

After the synthesis of stable SERS nanotag/antibody conjugates exhibiting a bright signal with sufficient stability suitable for single-particle SERS experiments, iSERS microscopy experiments were conducted on biological specimen [48]. The aim was to assess the applicability of iSERS for fast protein localization, reproducibility of the results [37] and multi-color experiments [16], since these aspects are crucial for possible future applications in clinical diagnostic methods. To gain a quick overview of the sample without performing time-consuming SERS mapping experiments, fluorophore labeled antibodies were employed to identify areas of interest for subsequent mapping [38].

3.1 Prostate tissue analysis with rapid two-color iSERS aided by protein A/G-AuNP-conjugates

Experiments investigating the feasibility of parallel staining of FFPE prostate tissue specimen with two different SERS nanotags were conducted by Salehi *et al* in 2014 [48]. SERS labels containing two different aromatic thiols were chosen as a SAM coating the surface: 4-NTB displays a Raman peak at about 1340 cm^{-1} due to the symmetric nitro stretching vibration, 4-MBA exhibits a Raman peak at about 1590 cm^{-1} due to a phenyl ring mode, rendering the spectra of these two Raman reporter molecules distinguishable from each other. Silica-coated trimers of 60 nm AuNPs were synthesized, as they exhibit single-particle sensitivity within 30 ms laser illumination (s. Section 2.4). To achieve molecular specificity and reliable detection results, successful binding of the targeted antigen by antigen-recognition sites of the antibody, the synthesis approach involving protein A/G coating of the NP shell was used. Antibody-protein A/G-AuNP trimers for detection of the basal cell marker p63 (4-MBA) and PSA (4-NTB) abundant in the whole prostate epithelium were used in single- and two-color immuno-SERS experiments.

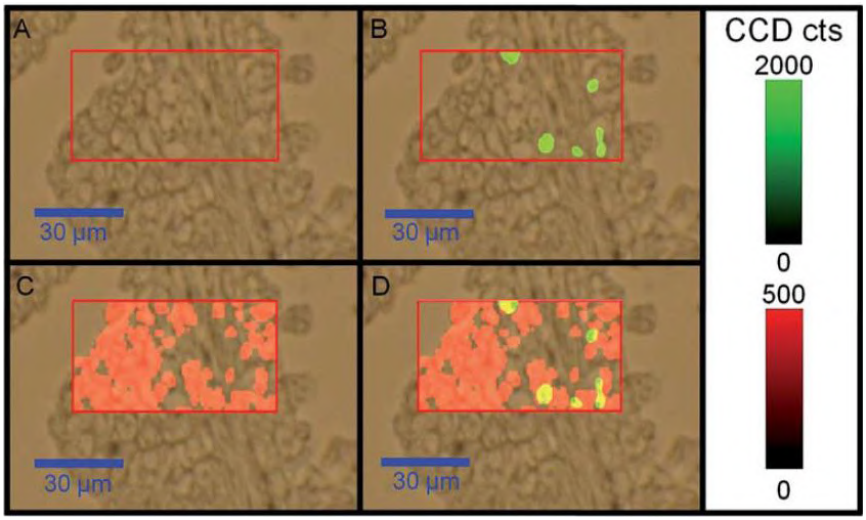

Fig 9. Overlay of white light images of prostate tissue with false-color SERS images from iSERS microscopy. Acquisition time: 100 ms per pixel. **A** White light image of a healthy prostate sample. **B** Overlay with a p63 (green) false-color SERS image (Raman reporter 4-MBA). **C** Overlay with a PSA (red) false-color SERS image (Raman reporter: 4-NTB). **D** Overlay to emphasize co-localization with p63/PSA SERS false-color images. From ref. [48].

First, single-color experiments were performed separately with both SERS nanotag/antibody conjugates to check their respective binding specificity. p63 could successfully be detected in the basal epithelium cells with SERS nanotags containing 4-MBA, while PSA was located in the epithelium of prostate

glands by SERS nanotags coated with 4-NTP (Fig 9). Furthermore, only minimal false-positive binding was evident in other areas as well as in experiments with negative controls. The two-color immuno-SERS experiments delivered the same results, the Raman bands of the two reporter molecules could successfully be separated from each other. Therefore, it could be demonstrated, that immuno-SERS, compared to standard IHC, shows a high potential regarding multiplexing in combination with high sensitivity [48].

3.2 Correlative iSERS microscopy and wide field immunofluorescence on human FFPE tissue

Measurements performed with normal Raman microscopy (mapping) typically require long acquisition times in the range of seconds per pixel, while samples investigated with confocal IF laser scanning only need microseconds of laser exposure for sufficient data acquisition. With bright SERS nanotags this gap could already be diminished to the millisecond range per pixel, but not yet closed. Therefore, the analysis of large biological specimen, such as entire tissue slides, with iSERS requires long mapping experiments and approaches rendering this technique more time-efficient need to be developed. In 2016 our group developed an approach to combine iSERS with immunofluorescence (IF) for fast investigation of large tissue sections followed by subsequent iSERS mapping experiments in smaller areas of interest [38]. This dual mode IF/iSERS approach was applied to breast tissue sections targeting the human epidermal growth factor receptor 2 (HER2). HER2 is involved in the regulation of cellular signaling in cell growth and development and serves as an important diagnostic biomarker for breast cancer. In 10-20% of breast cancer subtypes overexpression of HER2 can be recognized [49]. The SERS nanotags in these experiments consisted of gold nanostars hydrophilically stabilized by a coat of 4-NTB conjugated to MEG-OH or TEG-COOH. The NPs were then conjugated to Alexa647-labelled secondary antibodies at their carboxy-moiety. The conjugates were therefore both fluorescence- and SERS-active. The breast tissue sections were first deparaffinized and, after enzymatic antigen retrieval, incubated with unlabeled anti-HER2 primary antibodies. After removal of excess primary antibody, the tissue sections were incubated with the Alexa-647-/AuNP-conjugated secondary antibody for further analysis. Wide field IF was employed to gain a quick overview about antigen-presence on the tissue surface to guide SERS mapping of smaller areas.

SEM imaging of the SERS nanotags revealed relatively monodisperse Au nanostars with an average size of about 75 nm, but variable core diameter and number of tips per star. Then, IHC as the gold standard for clinical tissue analysis was compared to correlative bright field/IF/iSERS. Most cells on HER2-positive breast cancer cells exhibited staining, whereas no staining of cell membranes on normal breast tissue was observed. The results from correlative bright field/IF/iSERS-experiments also exhibited selective staining of cell membranes of cancerous cells only (Fig 10). The areas of interest covered in the bright field/IF/iSERS imaging experiments include the cell membrane, cytoplasm and extracellular regions. Only in cell membranes of HER2-positive tumor cells a Raman signal could be detected. To confirm the specificity of this method, two negative control experiments were performed: i) without the unlabeled primary antibody, but with the SERS-labeled secondary antibody and ii) with an isotope secondary antibody conjugated to the SERS nanotag, which is not recognizing the unlabeled primary antibody. In each negative control experiment no false-positive binding was detected. These experiments were performed again after 51 days and the capability of this staining method for longer storage and re-inspection was demonstrated [38]. Both imaging techniques, IF and iSERS microscopy, prove sensitive and selective binding, but iSERS still offers more potential due to its multiplexing and quantification possibilities. This could be especially helpful when investigating breast cancer, as reoccurring carcinomas are highly heterogeneous and their characterization aids successful therapeutic intervention in individualized therapies for patients [50,51].

In addition to cancer research also are diseases related to lifestyle. In this context, the Raman imaging group in Krakow, Poland, together with our group employed iSERS microscopy for the localization of smooth muscle cells (SMCs) in atherosclerotic plaques. [52]

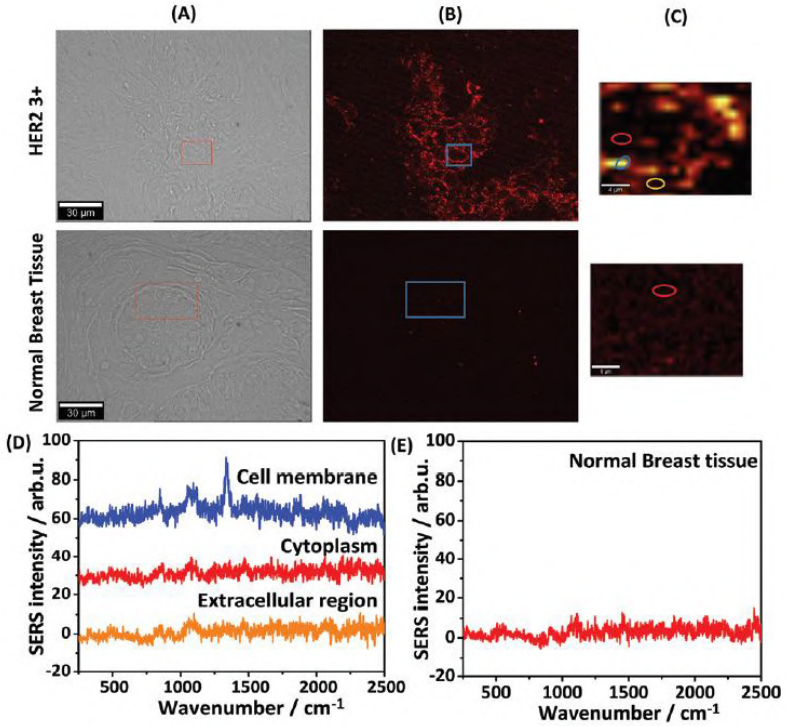

Fig 10. Bright field, IF and SERS microscopy images of breast cancer tissue and healthy breast tissue stained with antibody-conjugated gold nanostars. (A) Bright field image. (B) Immunofluorescence. (C) iSERS false-color images of areas marked in (A) and (B) (color scale: 30-300 CCD counts). (D) Raman spectra of different regions on HER2 positive breast cancer tissue. (E) Raman spectrum of healthy tissue. From ref. [38].

3.3 Fast and reproducible iSERS microscopy on HER2-positive human breast cancer cells

Increasing the laser power in iSERS imaging experiments for reducing the overall acquisition time is not recommended since the SERS nanotags are susceptible to photodamage [53]. This is critical when repeated measurements on the same specimen have to be performed. In 2017, X. Wang *et al*. investigated the influence of different laser power intensities and acquisition times on SERS signal intensity and reproducibility of the results [37]. The experiments were conducted on glass slides with fixated cells from the human breast cancer cell line SkBr3, which is a HER2-positive breast cancer cell line. MCF-7 cells served as the negative control. The SERS tag consisted of Raman reporter-labeled gold nanostars conjugated to anti-HER2 mouse antibodies. The fluorophore Alexa647 for wide field fluorescence microscopy was bound to a secondary goat anti-mouse antibody. Single cells were investigated repeatedly up to four times, while the used laser powers for sample investigation ranged from 0.49 mW to17.9 mW and the tested integration times per pixel were in a range of 0.05 to 0.8 s. High laser powers of 17.9 mW and 10.3 mW resulted in significantly decreased SERS signals already in the second run, therefore, these conditions are not suitable for reproducible measurements. As the Raman signal intensity is proportional to both the laser power and integration time, longer acquisition times were considered to compensate the further reduction of the laser power. After a reduction to 4.7 mW laser power, 0.4 s were sufficient for acquiring images with SERS signals above the detection limit and producing reproducible results for three times. Another option to increase the signal intensity was the gain function of the EMCCD. The combination of low laser power, millisecond acquisition time and high EM

gain yielded reproducible images. At an acquisition time of 50 ms a reduction of the laser power to 1.24 mW or even 0.49 mW gave signals high enough for a detection even in the fourth run (Fig 11). Further decrease in laser power lead to a lower signal to noise ratio and the fluorescence signals interfered with the spectra. Therefore, it can be concluded, that the combination of low laser power, short integration times per pixel and increased EMCCD gain enable reproducible SERS imaging with sufficient signal intensity.

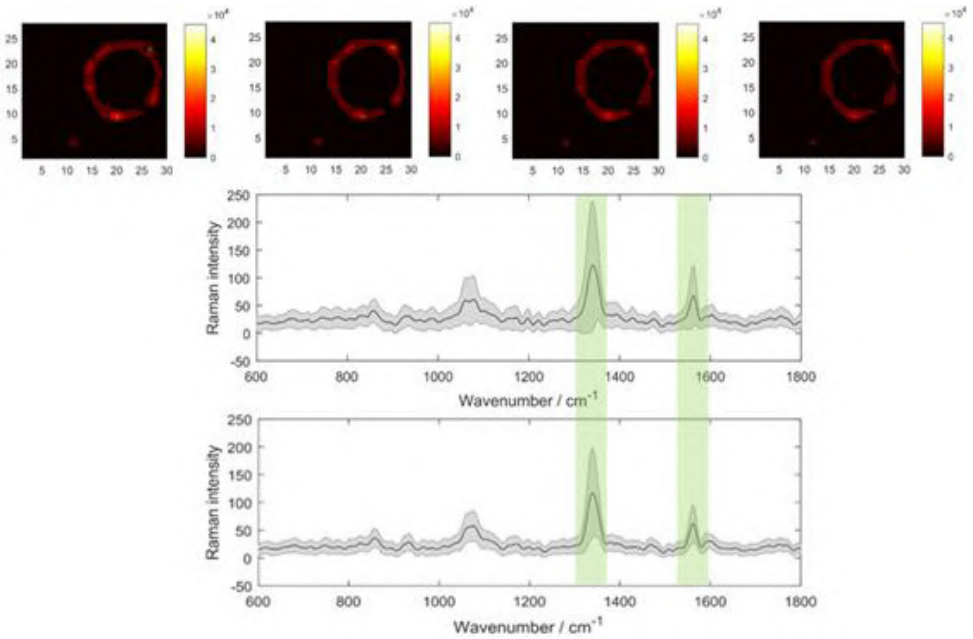

Fig 11. Repeated iSERS experiments on the same single cell with 2.3 mW laser power, EM gain 200 and 0.05 s acquisition time. Below: Baseline-corrected SERS spectra between the first (top) and the fourth (bottom) measurement. From ref. [37].

In addition to imaging of the breast cancer marker HER2 we also employed the same cancer cell line for selective imaging of programmed cell death-ligand 1 (PD-L1), which plays a crucial role in immune regulation [43].

3.4 Comparison of the influences of antigen retrieval methods on NP-binding

The staining quality in iSERS experiments (nonspecific binding, overall SERS signal level) is influenced by the efficiency of antigen retrieval on FFPE tissue slides. In 2017, Zhang *et al* tested different antigen retrieval methods and their effect on nonspecific binding of the NPs [54]. The SERS labels used in this study consisted of ca. 70 nm gold nanostars coated with ethylene glycol-bound Raman reporters, as ethylene glycols resemble a biocompatible polymer hydrophilically stabilizing the NP and exhibit only a low affinity to proteins. The NPs were conjugated to anti-PSA antibodies and tested on FFPE human prostate tissue sections treated with either heat-induced (HIER) or protease-induced epitope retrieval (PIER) [55]. Here, the HIER consisted of heating the rehydrated tissue sample in citrate (pH 6.0) or in EDTA buffer (pH 8.5) for 20 min to 96 °C and subsequent cooling in the same buffer for 20 min. In PIER a drop of fast enzyme is applied to the tissue specimen and incubated at RT for 5 min. The mechanism of formalin fixation and as well of antigen retrieval is yet to be understood, but a prominent speculation is that formalin-induced cross-linkages can be broken by heat and peptide bonds can be cleaved by enzymes [56]. In classic IHC, antigens can be retrieved more efficiently with one of the two methods and best results have to be investigated individually.

Both IF and SERS were performed on the human prostate tissue slides. IF exhibited the same fluorescence signal intensities treated with HIER and PIER, but the samples treated with PIER exhibited more uniform distributions, while the samples treated with HIER the staining was uneven with brighter spots and weaker regions. The iSERS experiments revealed a difference between HIER and PIER treated slides: the signal intensity when PSA could be detected, was equally bright, but in the negative control samples nonspecific binding of SERS labels was visible when treated with HIER. Moreover, when NPs were either conjugated to primary anti-PSA or secondary antibodies, nonspecific binding of NPs incubated with tissue slides treated with HIER was observed (Fig 12). To test if these effects also occur in other tissues, immunostaining of breast tissue sections with SERS nanotags binding HER2 were performed and exhibited nonspecific binding in samples treated with HIER as well. Moreover, the signal intensity detected on tissue slides treated with PIER were higher, offering more specific staining and better image contrast. Therefore, it can be concluded that the staining of prostate and breast tissue with gold nanostars was strongly affected by the chosen antigen retrieval method, as HIER induces nonspecific adsorption and more uneven NP distribution compared to tissue treated with PIER.

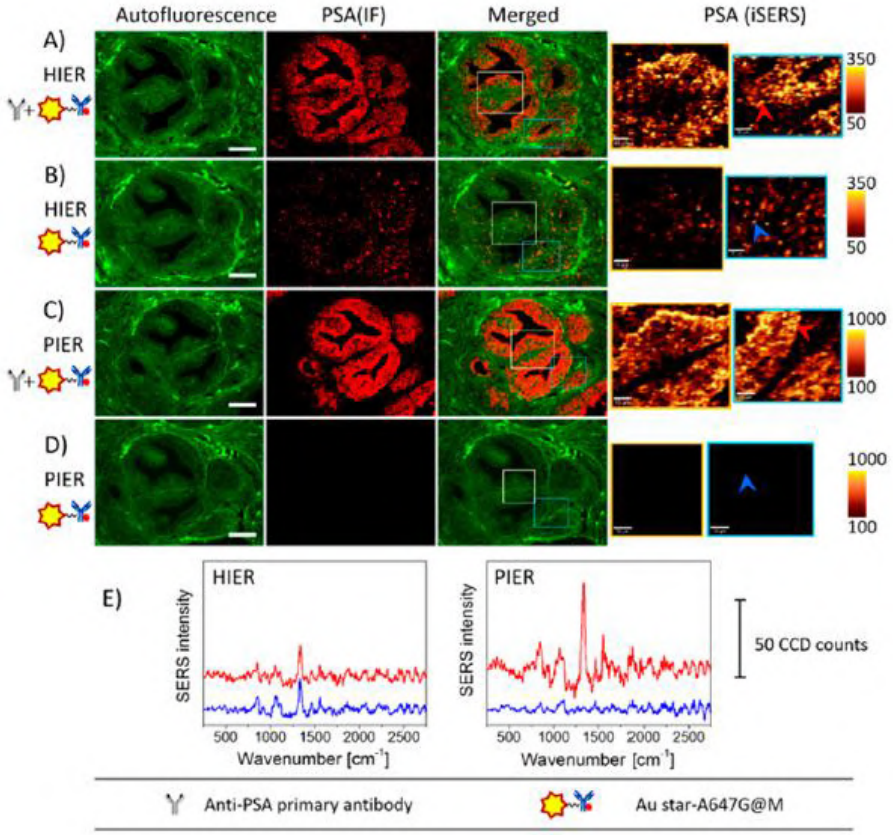

Fig 12. Comparison of HIER and PIER as antigen retrieval methods regarding their influence on the staining quality in indirect staining experiments. FFPE prostate tissue was treated with one of the chosen antigen retrieval methods and incubated with primary anti-PSA antibodies. For correlative IF/iSERS imaging, gold nanostars were conjugated to fluorophore-labeled secondary antibodies. (A) Results with HIER and (B) negative control without the primary anti-PSA antibody. (C) PIER and (D) negative control without the primary antibody. (E) Left: representative SERS spectra obtained in panels A and B. Right: SERS spectra obtained in panels C and D. Red and blue arrows indicate the location where the SERS spectra were acquired. Scale bar in fluorescence images: 50 µm. Scale bar in SERS images: 10 µm. From ref. [54].

To further investigate this effect, the nonspecific binding of the gold nanostar/antibody conjugates was compared to experiments performed with 20 nm spherical AuNPs. Tissue samples heated both in citrate or EDTA buffer exhibited similar nonspecific binding patterns for both SERS tags. Untreated tissue samples did not exhibit nonspecific binding. Furthermore, direct and indirect stainings with a secondary antibody were performed to test if PEG coating containing longer ethylene glycol units than the MEG/TEG-shell, improves the binding efficiency. It was observed that nonspecific binding could be reduced successfully, however the overall SERS signal intensity was weaker. The PEGylated SERS nanotags did not exhibit a complete dual-SAM, which lead to lower Raman band intensities. Moreover, the PEG coating increased the diameter of the probes to about 12 nm, which is also unfavorable for tissue staining as the size of NPs can be a steric hindrance for effective antigen recognition. This leads to the conclusion that PIER should be favored over HIER as an antigen retrieval method for iSERS experiments on FFPE tissue slides. If the targeted antigen cannot be retrieved efficiently with PIER, a combination of HIER and PEGylated SERS nanotags could be considered to reduce nonspecific interactions [54].

3.5 6-color/1-target iSERS microscopy on single cancer cells

Localization of multiple biomarkers is crucial for a comprehensive characterization of cancer cells at the single-cell level and for analyzing the heterogeneity at the population-level [57,58]. However, other optical bioimaging techniques, such as conventional immunofluorescence, lack the necessary multicolor capacity and suffer from disturbing autofluorescence [2,3]. Both these drawbacks can be circumnavigated by SERS using red to near-infrared laser excitation [59]. For demonstrating the proof of concept of using 6 spectrally distinct SERS nanotags on the same single cancer cell, we decided to localize the tumor marker HER2 by conjugating all different tags (Au/Au core/satellite particles with six distinct Raman reporter molecules on the Au core) to the same anti-HER2 antibody [16]. A comparable SERS signal intensity from all six nanotags was achieved by a combination of tunable core size for controlling core/satellite plasmon coupling and Raman reporter-specific adsorption conditions for each SERS nanotag. Breast cancer cells (SkBr-3) overexpressing HER2 were incubated with a mixture of all six antibody-SERS nanotag conjugates and then analyzed by confocal Raman microscopy. A spectrum was recorded for each pixel during the Raman mapping experiments on single cells. Due to the specific recognition of the HER2 antigen by the anti-HER2 antibody, all SERS nanotag/anti-HER2 antibody conjugates selectively bound to HER2 localized on the cell membrane (Fig 13). These 6-color/1-target iSERS microscopic experiments on single SkBr-3 cells pave the way for future studies localizing a panel of six different targets on either the same cell or on a mixture of several/many single cells One area of our future research will be the use of iSERS for characterizing disseminated tumor cells in the bone marrow of breast cancer patients.

3.6 The importance of negative control experiments in iSERS staining

A crucial aspect of assessing the reliability of the obtained results is to test for false-positive binding of the antibody on the sample. Gold nanoparticles and antibodies can be subject to non-specific interactions with the tissue or cell surfaces [60]. Furthermore, antigen retrieval methods, NP shell composition and the size of the SERS nanotag influence the probability of the construct “sticking” to the sample surface [61]. It is, therefore, obligatory to question the influence of non-specific interactions on the overall SERS signal intensity. Experiments with isotype controls serve as a powerful tool regarding this issue. Isotype controls are primary antibodies without the specificity for the chosen target but match the class and type of the primary antibody used in the experiment. Signals from specific binding, therefore, can be differentiated from non-specific background signals and interactions between the sample and the SERS nanotag can be investigated [62]. In experiments conducted with primary and secondary antibodies, leaving out the staining with primary antibodies can serve as a negative control experiment. Moreover, cell lines not expressing the chosen antigen serve as another form of negative control [63]. The difference in SERS signal intensities between the overexpressing and the knockout cell line determines the significance of the results obtained

with the chosen staining method. Results obtained without questioning the significance of the data critically are not providing reliable information about the efficiency of this staining technique.

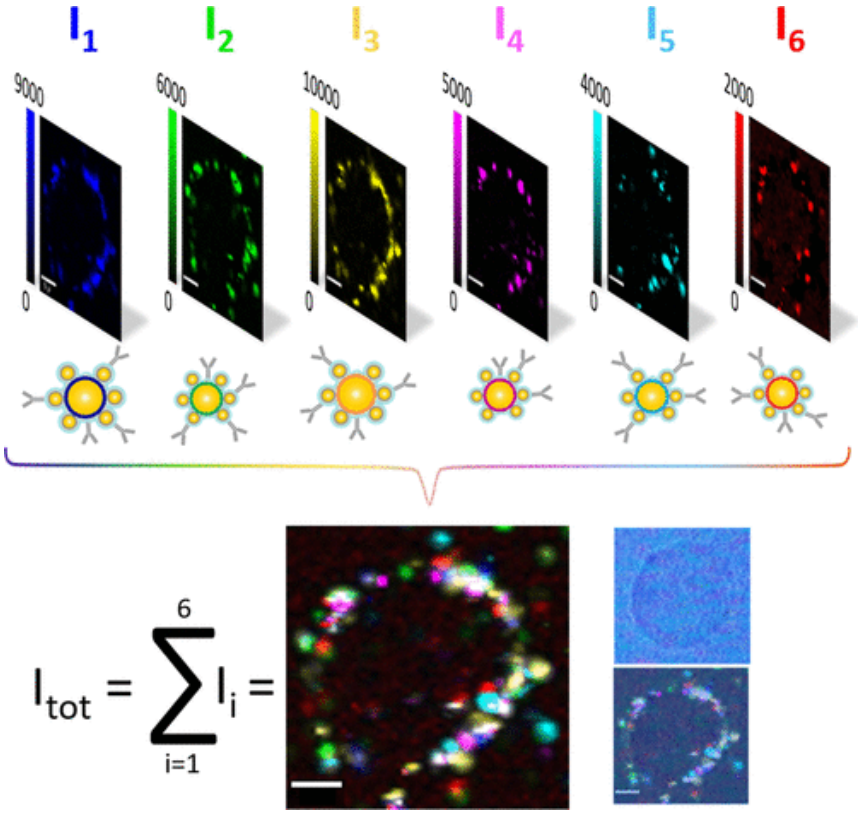

Fig 13. Multi-color iSERS microscopy on a single fixed (dead) SkBr-3 cancer cell incubated with six spectrally distinct SERS nanotags-antibody conjugates: For each pixel the individual intensity contributions from the tags to the recorded spectrum were determined by spectral decomposition using a least-square algorithm. A separate false color was assigned to each of the six nanotags. The final image I_{tot} is six individual false-color SERS images I_1 to I_6 of single cells, image I_1 shows the localization of HER2 revealed by the spectral barcode of the first SERS nanotag while image I_2 shows the localization of HER2 revealed by the spectral barcode of the second nanotag and so forth. From ref. [16].

4 Conclusion

In this contribution the development of SERS nanotags, stabilized for reproducibility and decreased in size for efficient antigen recognition while maintaining sufficient field enhancement of the Raman reporter signal, was explained. This leads to fast and reproducible iSERS experiments on cells and tissue specimen. With the development of highly plasmonically active NPs like gold nanostars and core/satellite-suprastructures containing “hot spots”, the signal intensity was enhanced, thereby enabling measurements at the single-particle level. This also led to a reduction in acquisition times from 1 s to 30 ms, rendering this imaging technique more applicable for clinical use. Moreover, the combination of SERS nanotags with fluorophore-labeled antibodies enabled the rapid global analysis of large sample areas by wide-field immunofluorescence followed by local analysis of selected regions of interest by iSERS. Very recently, our group demonstrated a 6-plex/1-target iSERS experiment on the same single cancer cell. Future studies should

aim at multi-color/multi-target iSERS imaging of single cells and tissue sections. A lot of work remains to be done in the future, which will experimentally demonstrate the potential of iSERS compared to other competing optical techniques, in particular immunofluorescence with molecular fluorophores and quantum dots. Overall, we feel that the future for iSERS is bright and we encourage young scientists to apply this emerging nanobiophotonic technique for addressing challenges in biomedical sciences.

5 Acknowledgement

The work presented here was only possible due to the contributions of many former group members and collaboration partners. Their names are listed as coauthors of the corresponding papers in the reference section. The corresponding author is grateful for receiving the **Dayawati Rastogi Lecture Award** 2018 by the *Indian Spectroscopy Society* and the *Asian Journal of Physics*, which was conferred during the VII International Conference on Perspectives in Vibrational Spectroscopy (ICOPVS-2018) at BARC in Mumbai, India.

References

1. Langer J, Jimenez de Aberasturi D, Aizpurua J, Alvarez-Puebla R A, Auguié B, Baumberg J J, Bazan G C, Bell S E J, Boisen A, Brolo A G, Choo J, Cialla-May D, Deckert V, Fabris L, Faulds K, De Abajo FJG, Goodacre R, Graham D, Haes A J, Huck C L H C, Itoh T, Käll M, Kneipp J, Kotov N A, Kuang H, Ru E C L, Lee H K, Li J F, Ling X Y, Maier S A, Mayerhöfer T, Moskovits M, Murakoshi K, Nam J M, Nie S, Ozaki Y, Pastoriza-Santos I, Perez-Juste J, Popp J, Pucci A, Reich S, Ren B, Schatz G C, Shegai T, Schlücker S, Tay L L, Thomas K G, Tian Z Q, Duyne R P V, Vo-Dinh T, Wang Y, Willets K A, Xu C, Xu H, Xu Y, Yamamoto Y S, Zhao B, Liz-Marzán L M, Present and Future of Surface-Enhanced Raman Scattering, *ACS Nano*, 14(2020)28-117.
2. Schlücker S, SERS Microscopy: Nanoparticle Probes and Biomedical Applications. *Chem Phys Chem*, 10(2009) 1344-1354.
3. Schlücker S, Surface-Enhanced Raman Spectroscopy: Concepts and Chemical Applications, *Angew Chem Int Ed*, 53(2014)4756-4795.
4. Doering W E, Piotti M E, Natan M J, Freeman R G, SERS as a Foundation for Nanoscale, Optically Detected Biological Labels, *Adv Mater*, 19(2007)3100-3108.
5. Cao Y C, Jin R, Nam, J.-M, Thaxton C S, Mirkin C A, Raman Dye-Labeled Nanoparticle Probes for Proteins, *J Am Chem Soc*, 125(2003)14676-14677.
6. Cao Y C, Jin R, Mirkin C A, Nanoparticles with Raman Spectroscopic Fingerprints for DNA and RNA Detection, *Science*, 297(2002)1536.
7. Wang Y, Schlücker S, Rational design and synthesis of SERS labels, *Analyst*, 138(2013)2224-2238.
8. Gellner M, Kömpe K, Schlücker S, Multiplexing with SERS labels using mixed SAMs of Raman reporter molecules. *Anal Bioanal Chem*, 394(2009)1839-1844.
9. Le Ru EC, Etchegoin P G, Principles of surface-enhanced Raman spectroscopy: And related plasmonic effects,1st edn, (Elsevier, Amsterdam, Boston), 2009.
10. Feliu N, Hassan M, Garcia Rico E, Cui D, Parak W, Alvarez-Puebla R, SERS Quantification and Characterization of Proteins and Other Biomolecules, *Langmuir*, 33(2017)9711-9730.
11. Schütz M, Schlücker S, Towards quantitative multi-color nanodiagnostics: spectral multiplexing with six silica-encapsulated SERS labels, *J Raman Spectrosc*, 47(2016)1012-1016.
12. Tran V, Walkenfort B, König M, Salehi M, Schlücker S, Rapid, Quantitative, and Ultrasensitive Point-of-Care Testing: A Portable SERS Reader for Lateral Flow Assays in Clinical Chemistry, *Angew Chem Int Ed*, 58(2019) 442-446.
13. Schlücker S, Salehi M, Bergner G, Schütz M, Ströbel P, Marx A, Petersen I, Dietzek B, Popp J, Immuno-Surface-Enhanced Coherent Anti-Stokes Raman Scattering Microscopy: Immunohistochemistry with Target-Specific Metallic Nanoprobes and Nonlinear Raman Microscopy. *Anal Chem*, 83(2011)7081-7085.
14. Ni J, Lipert R J, Dawson G B, Porter M D, Immunoassay Readout Method Using Extrinsic Raman Labels Adsorbed on Immunogold Colloids. *Anal Chem*, 71(1999)4903-4908.

15. Schlücker S, Küstner B, Punge A, Bonfig R, Marx A, Ströbel P, Immuno-Raman microspectroscopy: In situ detection of antigens in tissue specimens by surface-enhanced Raman scattering. *J Raman Spectrosc*, 37(2006)719-721.
16. Stepula E, Wang X.-P, Srivastav S, König M, Levermann J, Kasimir-Bauer S, Schlücker S, 6-Color/1-Target Immuno-SERS Microscopy on the Same Single Cancer Cell, *ACS Appl Mater Interfaces*, 12(2020)32321-32327.
17. Gellner M, Küstner B, Schlücker S, Optical properties and SERS efficiency of tunable gold/silver nanoshells, *Vib Spectrosc*, 50(2009)43-47.
18. Stöber W, Fink A, Bohn E, Controlled growth of monodisperse silica spheres in the micron size range, *J Colloid Interface Sci*, 26(1968)62-69.
19. Schütz M, Küstner B, Bauer M, Schmuck C, Schlücker S, Synthesis of Glass-Coated SERS Nanoparticle Probes via SAMs with Terminal SiO_2 Precursors, *Small*, 6(2010)733-737.
20. Jehn C, Küstner B, Adam P, Marx A, Ströbel P, Schmuck C, Schlücker S, Water soluble SERS labels comprising a SAM with dual spacers for controlled bioconjugation, *Phys Chem Chem Phys*, 11(2009)7499-7504.
21. Schütz M, Salehi M, Schlücker S, Direct Silica Encapsulation of Self-Assembled-Monolayer-Based Surface-Enhanced Raman Scattering Labels with Complete Surface Coverage of Raman Reporters by Noncovalently Bound Silane Precursors, *Chem Asian J*, 9(2014)2219-2224.
22. Porter M D, Lipert R J, Siperko L M, Wang G, Narayanan R, SERS as a bioassay platform: fundamentals, design, and applications. *Chem Soc Rev*, 37(2008)1001-1011.
23. Niu W, Chua Y A A, Zhang W, Huang H, Lu X, Highly Symmetric Gold Nanostars: Crystallographic Control and Surface-Enhanced Raman Scattering Property, *J Am Chem Soc*, 137(2015)10460-10463.
24. Mulvihill M J, Ling X Y, Henzie J, Yang P, Anisotropic Etching of Silver Nanoparticles for Plasmonic Structures Capable of Single-Particle SERS, *J Am Chem Soc*, 132(2010)268-274.
25. Lin K.-Q, Yi J, Hu S, Liu B.-J, Liu J.-Y, Wang X, Ren B, Size Effect on SERS of Gold Nanorods Demonstrated via Single Nanoparticle Spectroscopy, *J Phys Chem C*, 120(2016)20806-20813.
26. Steinigeweg D, Schütz M, Schlücker S, Single gold trimers and 3D superstructures exhibit a polarization-independent SERS response, *Nanoscale*, 5(2013)110-113.
27. Zhang Y, Walkenfort B, Yoon J H, Schlücker S, Xie W, Gold and silver nanoparticle monomers are non-SERS-active: a negative experimental study with silica-encapsulated Raman-reporter-coated metal colloids. *Phys Chem Chem Phys*, 17(2015)21120-21126.
28. Gellner M, Steinigeweg D, Ichilmann S, Salehi M, Schütz M, Kömpe K, Haase M, Schlücker S, 3D Self-Assembled Plasmonic Superstructures of Gold Nanospheres: Synthesis and Characterization at the Single-Particle Level. *Small*, 7(2011)3445-3451.
29. Xie W, Walkenfort B, Schlücker S, Label-Free SERS Monitoring of Chemical Reactions Catalyzed by Small Gold Nanoparticles Using 3D Plasmonic Superstructures, *J Am Chem Soc*, 135(2013)1657-1660.
30. Xie W, Schlücker S, Hot electron-induced reduction of small molecules on photorecycling metal surfaces. *Nature Communications*, 6(2015)7570; doi.org/10.1038/ncomms8570.
31. Salehi M, Steinigeweg D, Ströbel P, Marx A, Packeisen J, Schlücker S, Rapid immuno-SERS microscopy for tissue imaging with single-nanoparticle sensitivity, *J Biophotonics*, 6(2013)785-792.
32. Tran V, Thiel C, Svejda J T, Jalali M, Walkenfort B, Erni D, Schlücker S, Probing the SERS brightness of individual Au nanoparticles, hollow Au/Ag nanoshells, Au nanostars and Au core/Au satellite particles: single-particle experiments and computer simulations. *Nanoscale*, 10(2018)21721-21731.
33. Pilot R, Signorini R, Durante C, Orian L, Bhamidipati M, Fabris L, A Review on Surface-Enhanced Raman Scattering. *Biosensors*, (*Basel*), 9(2019)57; doi.org/10.3390/bios9020057.
34. Qian X, Li J, Nie S, Stimuli-Responsive SERS Nanoparticles: Conformational Control of Plasmonic Coupling and Surface Raman Enhancement. *J Am Chem Soc*, 131(2009)7540-7541.
35. Li W, Camargo, P H C, Lu X, Xia Y, Dimers of Silver Nanospheres: Facile Synthesis and Their Use as Hot Spots for Surface-Enhanced Raman Scattering, *Nano Lett*, 9(2009)485-490.
36. König M, Radojcic A, Schlücker S, Xie W, Label-free SERS monitoring of hydride reduction catalyzed by Au nanostars, *J Raman Spectrosc*, 47(2016)1024-1028.

37. Wang X.-P, Walkenfort B, König M, König L, Kasimir-Bauer S, Schlücker S, Fast and reproducible iSERS microscopy of single HER2-positive breast cancer cells using gold nanostars as SERS nanotags, *Faraday Discuss*, 205(2017)377-386.
38. Wang X.-P, Zhang Y, König M, Papadopoulou E, Walkenfort B, Kasimir-Bauer S, Bankfalvi A, Schlücker S, iSERS microscopy guided by wide field immunofluorescence: analysis of HER2 expression on normal and breast cancer FFPE tissue sections, *Analyst*, 141(2016)5113-5119.
39. Stepula E, König M, Wang X.-P, Levermann J, Schimming T, Kasimir-Bauer S, Schilling B, Schlücker S, Localization of PD-L1 on single cancer cells by iSERS microscopy with Au/Au core/satellite nanoparticles, *J Biophotonics*, 13(2020)e201960034; doi.org/10.1002/jbio.201960034.
40. Schütz M, Müller C I, Salehi M, Lambert C, Schlücker S, Design and synthesis of Raman reporter molecules for tissue imaging by immuno-SERS microscopy, *J Biophotonics*, 4(2011)453-463.
41. Würthner F (ed), Supermolecular dye chemistry, (Springer: Berlin), 2005.
42. Love J C, Estroff L A, Kriebel J K, Nuzzo R G, Whitesides G M, Self-Assembled Monolayers of Thiolates on Metals as a Form of Nanotechnology, *Chem Rev*, 105(2005)1103-1170.
43. Keller T, Brem S, Tran V, Sritharan O, Schäfer D, Schlücker S, Rational design of thiolated polyenes as trifunctional Raman reporter molecules in surface-enhanced Raman scattering nanotags for cytokine detection in a lateral flow assay, *J Biophotonics*, 13(2020)e201960126; doi.org/10.1002/jbio.201960126.
44. Jazayeri M H, Amani H, Pourfatollah A A, Pazoki-Toroudi H, Sedighimoghaddam B, Various methods of gold nanoparticles (GNPs) conjugation to antibodies. *Sensing and Bio-Sensing Research*, 9(2016)17-22.
45. Yan Q, Zheng H.-N, Jiang C, Li K, Xiao S.-J, EDC/NHS activation mechanism of polymethacrylic acid: anhydride versus NHS-ester, *RSC Advances*, 5(2015)69939-69947.
46. Eliasson M, Andersson R, Olsson A, Wigzell H, Uhlén M, Differential IgG-binding characteristics of staphylococcal protein A, streptococcal protein G, and a chimeric protein AG, *J Immunol*, 142(1989)575-585.
47. Eliasson M, Olsson A, Palmcrantz E, Wiberg K, Inganäs M, Guss B, Lindberg M, Uhlén M, Chimeric IgG-binding receptors engineered from staphylococcal protein A and streptococcal protein G, *J Biol Chem*, 263(1988)4323-4327.
48. Salehi M, Schneider L, Ströbel P, Marx A, Packeisen J, Schlücker S, Two-color SERS microscopy for protein co-localization in prostate tissue with primary antibody–protein A/G–gold nanocluster conjugates, *Nanoscale*, 6(2014) 2361-2367.
49. Wolff A C, Hammond, M E H, Schwartz J N, Hagerty K L, Allred D C, Cote R J, Dowsett M, Fitzgibbons P L, Hanna, W M, Langer A, McShane L M, Paik S, Pegram M D, Perez E A, Press M F, Rhodes A, Sturgeon C, Taube S E, Tubbs R, Vance G H, Vijver M, Wheeler T M, Hayes D F, American Society of Clinical Oncology/ College of American Pathologists Guideline Recommendations for Human Epidermal Growth Factor Receptor 2 Testing in Breast Cancer, *J Clin Oncol*, 25(2007)118-145.
50. Kasimir-Bauer S, Hoffmann O, Wallwiener D, Kimmig R, Fehm T, Expression of stem cell and epithelial-mesenchymal transition markers in primary breast cancer patients with circulating tumor cells. *Breast Cancer Research*, 14(2012) R15; doi.org/10.1186/bcr3099.
51. Jeibouei S, Akbari M E, Kalbasi A, Aref A R, Ajoudanian M, Rezvani A, Zali H, Personalized medicine in breast cancer: pharmacogenomics approaches. *Pharmgenomics Pers Med*, 12(2019)59-73.
52. Wiercigroch E, Stepula E, Mateuszuk L, Zhang Y, Baranska M, Chlopicki S, Schlücker S, Malek K, Immuno SERS microscopy for the detection of smooth muscle cells in atherosclerotic plaques, *Biosensors and Bioelectronics*, 133(2019)79-85.
53. Zhang Y, Qiu Y, Lin L, Gu H, Xiao Z, Ye J, Ultraphotostable Mesoporous Silica-Coated Gap-Enhanced Raman Tags (GERTs) for High-Speed Bioimaging, *ACS Applied Materials & Interfaces*, 9(2017)3995-4005.
54. Zhang Y, Wang X.-P, Perner S, Bankfalvi A, Schlücker S, Effect of Antigen Retrieval Methods on Nonspecific Binding of Antibody–Metal Nanoparticle Conjugates on Formalin-Fixed Paraffin-Embedded Tissue, *Anal Chem*, 90(2018)760-768.
55. Shi S-R, Shi Y, Taylor C R, Antigen retrieval immunohistochemistry: review and future prospects in research and diagnosis over two decades, *J Histochem Cytochem*, 59(2011)13-32.

56. Kabiraj A, Gupta J, Khaitan T, Bhattacharya P T, Principle and techniques of immunohistochemstry - a review. *Int J Biol Med Res*, 6(2015)5204-5210.
57. Lim S B, Lim C T, Lim W.-T, Single-Cell Analysis of Circulating Tumor Cells: Why Heterogeneity Matters, *Cancers* (*Basel*), 11(2019)595; doi.org/10.3390/cancers11101595
58. Rossi E, Zamarchi R, Single-Cell Analysis of Circulating Tumor Cells: How Far Have We Come in the -Omics Era? *Front Genet* , 10(2019)958; doi.org/10.3389/fgene.2019.00958.
59. Liu R, Zhao J, Han G, Zhao T, Zhang R, Liu B, Liu Z, Zhang C, Yang L, Zhang Z, Click-Functionalized SERS Nanoprobes with Improved Labeling Efficiency and Capability for Cancer Cell Imaging, *ACS Appl Mater Interfaces*, 9(2017)38222-38229.
60. Schneider C S, Perez J G, Cheng E, Zhang C, Mastorakos P, Hanes J, Winkles J A, Woodworth G F, Kim A J, Minimizing the non-specific binding of nanoparticles to the brain enables active targeting of Fn14-positive glioblastoma cells, *Biomaterials*, 42(2015)42-51.
61. Bentzen E L, Tomlinson I D, Mason J, Gresch P, Warnement M R, Wright D, Sanders-Bush E, Blakely R, Rosenthal S J, Surface Modification To Reduce Nonspecific Binding of Quantum Dots in Live Cell Assays, *Bioconjugate Chem*, 16(2005)1488-1494.
62. Andersen M N, Al-Karradi S N H, Kragstrup T W, Hokland M, Elimination of erroneous results in flow cytometry caused by antibody binding to Fc receptors on human monocytes and macrophages, *Cytometry A*, 89(2016)1001-1009.
63. Torlakovic E E, Francis G, Garratt J, Gilks B, Hyjek E, Ibrahim M, Miller R, Nielsen S, Petcu E B, Swanson P E, Taylor C R, Vyberg M, Standardization of negative controls in diagnostic immunohistochemistry: recommendations from the international ad hoc expert panel, *Appl Immunohistochem Mol Morphol*, 22(2014)241-252.

[*Received*: 05.09.2020; *accepted*: 10.09.2020]

Michelle Hechler joined the Schlücker group at the University Duisburg-Essen, Germany, as a Ph D student in 2019 for obtaining her doctoral degree in physical chemistry, supported by the German Cancer Aid. She completed her Master´s degree in medical biology. Her research interests include the synthesis and biological applications of gold nanoparticles, in particular for cell-based cancer diagnostics.

Supriya Srivastav is a postdoctoral researcher in the Schlücker group at the Department of Chemistry, University of Duisburg-Essen, Germany. She graduated with a Ph D in Biochemistry in 2013 from CSIR-Indian Institute of Chemical Biology (University of Calcutta), Kolkata, India, a M Sc in Zoology and a specialization in Biochemistry from Banaras Hindu University (BHU) in Varanasi, India, in 2007. Her current research interests are cell biology, breast cancer and immuno-SERS microscopy with an emphasis of protein identification and localization at the single-cell level.

Sebastian Schlücker is a Professor of Physical Chemistry at the Department of Chemistry, University of Duisburg-Essen, in Essen, Germany. He obtained his Ph D. in Physical Chemistry from the University of Würzburg under the guidance of Wolfgang Kiefer in 2002 and postdoctoral training at the Laboratory of Chemical Physics at NIH in Bethesda, MD, USA. His research interests are the development of innovative Raman spectroscopic and microscopic techniques for chemical and biomedical applications as well as the physics and chemistry of molecularly functionalized noble metal nanoparticles.